Inorg. Chem. **2002**, *41*, 6514–6520

Structures of Novel $R_2Mo_5O_{18}$ and $R_6Mo_{12}O_{45}$ (R = Eu and Gd) Prepared by Thermal Decomposition of Polyoxomolybdate Precursor $[R_2(H_2O)_{12}Mo_8O_{27}]\cdot nH_2O$

Haruo Naruke* and Toshihiro Yamase

Chemical Resources Laboratory, Tokyo Institute of Technology, 4259 Nagatsuta, Midori-ku Yokohama 226-8503, Japan

Received May 7, 2002

Single crystals of $R_2Mo_5O_{18}$ and $R_6Mo_{12}O_{45}$ (R = Eu and Gd), which are novel compounds in the R_2O_3–MoO_3 system, have been obtained by thermal decomposition of $[R_2(H_2O)_{12}Mo_8O_{27}]\cdot nH_2O$ in air at 750 °C for 2 h. TG-DTA and X-ray diffractometry showed that $R_2Mo_5O_{18}$ crystallizes in a melt of the dehydrated precursor ($R_2Mo_8O_{27}$), and $R_2Mo_5O_{18}$ is transformed to $R_6Mo_{12}O_{45}$ in the solid state, both occurring with the loss of MoO_3. $R_2Mo_5O_{18}$ species crystallize isostructurallyas orthorhombic, *Pbcn*, $Z = 4$, with lattice constants of $a = 19.2612(7)$ and 19.246-(1) Å, $b = 9.4618(3)$ and 9.4414(5) Å, $c = 9.3779(3)$ and 9.3446(4) Å for R = Eu and Gd, respectively. $R_6Mo_{12}O_{45}$ crystallize isostructurally as triclinic $P\bar{1}$, $Z = 1$, with lattice constants of $a = 9.3867(4)$ and 9.3409(3) Å, $b = 10.9408(5)$ and 10.8826(5) Å, $c = 11.4817(5)$ and 11.4377(5) Å, $\alpha = 104.194(2)°$ and 104.170(1)°, $\beta = 109.567(3)°$ and 109.288(4)°, $\gamma = 108.998(2)°$ and 109.266(2)° for R = Eu and Gd, respectively. Both structures consist of $\{RO_8\}$ square-antiprisms and $\{MoO_n\}$ polyhedra. In $R_2Mo_5O_{18}$, an $\{RO_8\}$ polyhedron is attached by only molybdate groups, being isolated from adjacent $\{RO_8\}$ groups. The 12 nearest R atoms surrounding an R atom with R···R distances of 6.0735(4)–7.0389(4) Å form an approximate cuboctahedron. All the $\{RO_8\}$ square-antiprisms in $R_6Mo_{12}O_{45}$ are connected to each other by face-sharing to form dimeric $\{R_2O_{13}\}$ and $\{R_2O_{12}\}$ groups. The latter unusual $\{R_2O_{12}\}$ group is achieved by sharing a square-face via four bridging O atoms with a very short R···R separation (3.4741(7) and 3.4502(6) Å for R = Eu and Gd, respectively).

Introduction

Solid-state materials based on rare earth molybdates, $R_2(MoO_4)_3$ and R_2MoO_6 (R = rare earth elements), have attracted much interest, because of their remarkable properties such as ferroelectricity and ferroelasticity,[1] laser hosts,[2] phosphors,[3] and catalysis.[4] The former $R_2(MoO_4)_3$ and related compounds have also been studied for their trivalent R ion conduction[5] and unusual thermal expansion behavior.[6] Most of the structural studies of rare earth molybdates $mR_2O_3\cdot nMoO_3$ are therefore concentrated on these two compounds ($m:n = 1:3$[7] and 1:1,[8] respectively), and very little is known about other $m:n$ compositions. A recent discovery of fast oxide ion conduction in $La_2Mo_2O_9$ ($m:n = 1:2$)[9] and its structure determination[10] stimulated us to further investigation of the structures and properties of $mR_2O_3\cdot nMoO_3$ with other $m:n$ compositions and various R species.

* To whom correspondence should be addressed. E-mail: hnaruke@res.titech.ac.jp. Phone and fax: +81 (0)45-924-5271.

(1) Aizu, K.; Kumada, A.; Yumoto, H.; Ashida, S. *J. Phys. Soc. Jpn.* **1969**, *27*, 511.
(2) Borchardt, H. J.; Bierstedt, P. E. *Appl. Phys. Lett.* **1966**, *8*, 50−52.
(3) Blasse, G.; Bril, A. *J. Chem. Phys.* **1966**, *45*, 2350. (b) Ouwerkerk, M.; Kellendonk, F.; Blasse, G. *J. Chem. Soc., Faraday Trans. 2* **1982**, *78*, 603. (c) Huang, J.; Lories, J.; Porcher, P. *J. Solid State Chem.* **1982**, *73*, 87.
(4) Xue, J. S.; Antonio, M. R.; Soderholm, L. *Chem. Mater.* **1995**, *7*, 333.
(5) Imanaka, N.; Ueda, T.; Okazaki, Y.; Tamura, S.; Adachi, G. *Chem. Mater.* **2000**, *12*, 1910.
(6) Evans, J. S. O.; Marry, T. A.; Sleight, A. W. *J. Solid State Chem.* **1997**, *133*, 580.
(7) Jamison, P. B.; Abrahams, S. C.; Bernstein, J. L. *J. Chem. Phys.* **1969**, *50*, 86. (b) Keve, E. T.; Abrahams, S. C.; Bernstein, J. L. *J. Chem. Phys.* **1971**, *54*, 3185. (c) Jeischko, W. *Acta Crystallogr.* **1973**, *B29*, 2074. (d) Abrahams, S. C.; Svensson, C.; Bernstein, J. L. *J. Chem. Phys.* **1980**, *72*, 4278.
(8) Klevtsov, P. V.; Kharchenko, L. Y.; Klevtsova, R. F. *Sov. Phys. Crystallogr.* **1975**, *20*, 349. (b) Efremov, V. A.; Tyunlin, A. V.; Trunov, V. K. *Sov. J. Coord. Chem.* **1987**, *13*, 721.
(9) Lacorre, P.; Goutenoire, F.; Bohnke, O.; Retoux, R.; Laligant, Y. *Nature* **2000**, *404*, 856.
(10) Goutenoire, F.; Isnard, O.; Retoux, R.; Lacorre, P. *Chem. Mater.* **2000**, *12*, 2575.

10.1021/ic025697z CCC: $22.00
Published on Web 11/06/2002

The rare earth molybdates are conventionally prepared by firing stoichiometric mixtures of R_2O_3 and MoO_3.[11] The highest firing temperature is usually limited to ~650 °C in order to avoid vaporization of MoO_3, and a complete reaction requires a long firing time (for between one and several days). Because many of the rare earth molybdates are obtained in powder form (except for $R_2(MoO_4)_3$ and R_2MoO_6),[11] their structural determinations should be done with the help of powder X-ray or neutron diffraction methods.[4,10,12] Recently, we found that rapid thermal decomposition and melting of a rare earth polyoxomolybdate, $[R_2(H_2O)_{12}Mo_8O_{27}]\cdot nH_2O$ (R = Eu and Tb), at 750−800 °C gave single crystals of $Eu_4Mo_7O_{27}$, $Eu_6Mo_{10}O_{39}$,[13] and $Tb_2Mo_4O_{15}$.[14] The former two compositions (m:n= 2:7 or 3:10) were completely new phases in the $mR_2O_3\cdot nMoO_3$ system, and the last compound was isomorphous with $Ho_2Mo_4O_{15}$.[15] The precursor $[R_2(H_2O)_{12}Mo_8O_{27}]\cdot nH_2O$ consists of a γ-type octamolybdate polymer $\{(Mo_8O_{27})^{6-}\}_\infty$ attached by hexahydrated $[R(H_2O)_6]^{3+}$ cations and lattice water molecules,[16] which is considered to be a stoichiometric mixture of R_2O_3, MoO_3, and H_2O with a 1:8:(12+n) ratio dispersed at a molecular level. This preparation method is advantageous for the growth of relatively large (~1 mm) single crystals in a short firing time (2 h), although control of the stoichiometry is somewhat difficult because MoO_3 vaporizes during the reaction. In the present study, the decomposition process of $[R_2(H_2O)_{12}Mo_8O_{27}]\cdot nH_2O$ (R = Eu and Gd) was analyzed by means of thermogravimetry and differential thermal analyses. Also, this preparation method was applied to synthesize $R_2Mo_5O_{18}$ and $R_6Mo_{12}O_{45}$ (R = Eu and Gd). The former composition (m:n = 1:5) is the first observation in the $mR_2O_3\cdot nMoO_3$ (R = Eu and Gd) system, while the latter (m:n = 3:12) is structurally determined for the first time.

Experimental Section

Syntheses. The precursor polyoxomolybdoeuropate, $[Eu_2(H_2O)_{12}Mo_8O_{27}]\cdot 6H_2O$, was prepared by an improved method reported in ref 16. An aqueous solution (10 mL) containing MoO_3 (1.93 g, 13.4 mmol) and KOH (1.5 g, 26 mmol) was diluted to ~1000 mL with water and acidified to pH = 4.5 with $HClO_4$. $Eu(NO_3)_3\cdot 6H_2O$ (1.49 g, 3.34 mmol) was dissolved in water (20 mL) and added slowly to the molybdate solution with stirring at room temperature. The resulting solution was reacidified to pH = 3.0 with $HClO_4$ and kept at room temperature. Pale yellow water-insoluble powders of $[Eu_2(H_2O)_{12}Mo_8O_{27}]\cdot 6H_2O$ that formed after several days were collected by filtration, washed with water, and dried in air. The gadolinium analogue was obtained by the same synthesis procedure except for replacement of $Eu(NO_3)_3\cdot 6H_2O$ with $Gd(NO_3)_3\cdot 6H_2O$ (1.51 g, 3.35 mmol). Analyses by powder X-ray diffractometry, energy dispersion X-ray (EDX) fluorescence spectroscopy (JEOL, JSX-3200), and thermogravimetry showed that the gadolinium analogue has the formula $[Gd_2(H_2O)_{12}Mo_8O_{27}]\cdot\sim 8H_2O$ and is isostructural with the europium compound. Found: Gd, 16.2; Mo, 37.5; H_2O, 19.2 wt %. Calcd for $Gd_2Mo_8O_{27}(H_2O)_{20}$: Gd, 16.78; Mo, 40.95, H_2O, 19.21 wt %.

The powdered sample of the precursor, $[R_2(H_2O)_{12}Mo_8O_{27}]\cdot nH_2O$ (R = Eu and Gd) (0.1 g), on a boat-shaped alumina container was inserted in a 750 °C preheated furnace, maintained for 2 h, and then quenched by exposure to room temperature. The reaction conditions have been described in our previous paper[13] in greater detail. When the sample was fired on a virgin container, the product was a dark brown-green glassy substance containing no crystals. Repeated reactions (750 °C, 2 h) using the same container (the product was mechanically removed after each reaction) resulted in the growth of prismatic and/or thin-plate colorless crystals of $R_2Mo_5O_{18}$ in the glassy substance. The color of the melt was occasionally pale yellow. When the firing time was prolonged to 4 h, colorless block crystals of $R_6Mo_{12}O_{45}$ were partially formed in the $R_2Mo_5O_{18}$ crystals. The two species were clearly discriminated by IR spectroscopic (JASCO FT/IR-410) measurement (data are available as Supporting Information). The Mo/R ratios for the single crystals measured by EDX were in good agreement with the values on the basis of their structural formula: $Eu_2Mo_5O_{18}$, Mo/Eu = 2.5; $Gd_2Mo_5O_{18}$, Mo/Gd = 2.7; $Eu_6Mo_{12}O_{45}$, Mo/Eu = 1.9; $Gd_6Mo_{12}O_{45}$ Mo/Gd = 2.0.

Thermogravimetric and Differential Thermal Analyses (TG-DTA). A TG-DTA of the precursor was performed on the ULVAC MTS9000+TGD9600 system. Sample (40−50 mg) and reference (Al_2O_3) were placed in Pt-cells (diameter, 3 mm; depth, 3 mm), heated in air to 750 °C at a rate of 10 °C min^{-1}, and maintained for 2−4 h.

X-ray Diffraction. Single-crystal X-ray structure determination for $R_2Mo_5O_{18}$ and $R_6Mo_{12}O_{45}$ was performed using a Rigaku RAXIS−RAPID imaging-plate X-ray diffractometer with a graphite-monochromatized Mo Kα X-ray source (λ = 0.71069 Å). The single crystals were mounted on glass fibers and measured at 25 °C. All of the structures except for $Gd_6Mo_{12}O_{45}$ were solved by SIR92.[17] The initial atomic positions for $Gd_6Mo_{12}O_{45}$ were imported from the data for isostructural $Eu_6Mo_{12}O_{45}$. The structure refinement was performed on F^2 with the full-matrix least-squares method. Numerical absorption correction was done using SHAPE[18] and NUMABS.[19] Anisotropic thermal parameters and extinction coefficients were refined for all of the compounds. All structure analyses were done using TEXSAN software.[20] The crystal data and results of the structure refinement are given in Table 1. Selected interatomic distances and angles are listed in Tables 2 and 3, respectively.

Powder X-ray diffraction (XRD) was carried out on a Rigaku RINT Ultima+/PC with graphite-monochromatized Cu Kα (λ = 1.54184 Å) radiation. In the case where the sample amount is small, the sample was sealed in a glass capillary (diameter 0.3 mm), mounted on the imaging-plate diffractometer, and exposed to a 0.3 mm-collimated X-ray beam for 15 min. The resulting image of diffraction rings was integrated and converted into a 2θ versus intensity plot.

(11) Brixner, L. H.; Barkley, J. R.; Jeitschko, W. In *Handbook on the Physics and Chemistry of Rare Earths*; Geschneidner, K. A. Jr., Eyring, L., Eds.; North-Holland Publishing Co.: Amsterdam, 1979; Vol. 3, Chapter 30, p 610.
(12) Dubois, F.; Goutenoire, F.; Laligant, Y.; Suard, E.; Lacorre, P. *J. Solid State Chem.* **2001**, *159*, 228.
(13) Naruke, H.; Yamase, T. *J. Solid State Chem.* **2001**, *161*, 85.
(14) Naruke, H.; Yamase, T. *Acta Crystallogr.* **2001**, *E57*, i106.
(15) Efremov, V. A.; Davydova, N. N.; Gokhman, L. Z.; Evdokimov, A. A.; Trunov, V. K. *Russ. J. Inorg. Chem.* **1988**, *33*, 1732.
(16) Yamase, T.; Naruke, H. *J. Chem. Soc., Dalton Trans.* **1991**, 285.
(17) Altomare, A.; Burla, M. C.; Camalli, M.; Cascarano, M.; Giacovazzo, C.; Guagliardi, A.; Polidori, G. *J. Appl. Crystallogr.* **1994**, *27*, 435.
(18) Higashi, T. *SHAPE−Program to obtain Crystal Shape using CCD camera*; Rigaku Corporation: Tokyo, 1999.
(19) Higashi, T. *NUMABS−Numerical Absorption Correction*; Rigaku Corporation: Tokyo, 1999.
(20) *TEXSAN, Single-Crystal X-ray Crystallographic Analysis Software*; version 1.11; Molecular Structure Corporation, MSC: The Woodlands, TX, 2000.

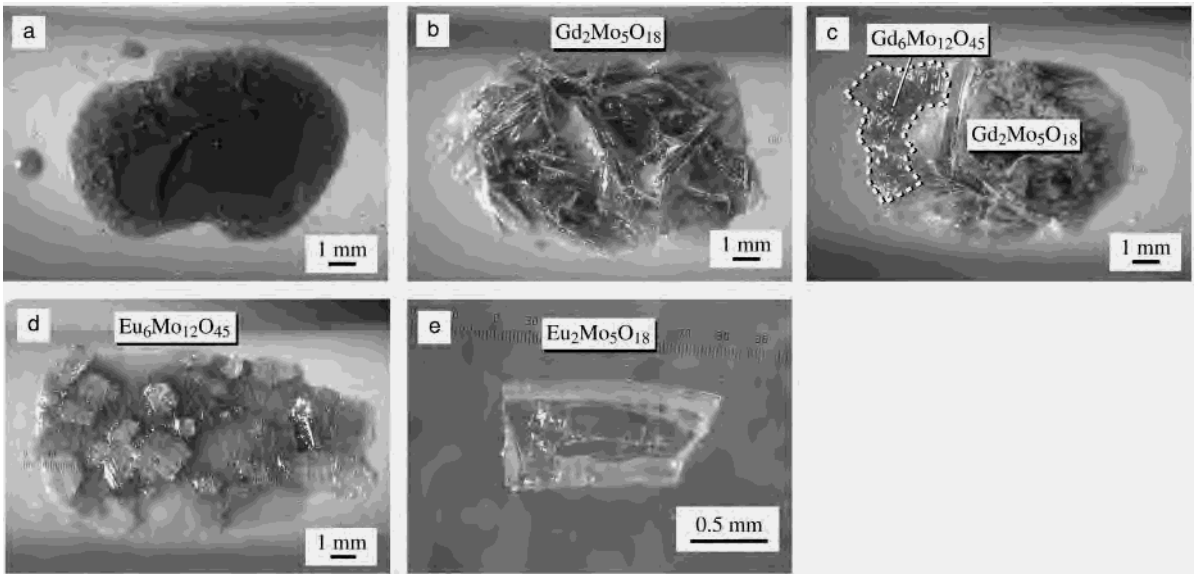

Figure 1. Microscopic images of the thermal decomposition products obtained by firing $[R_2(H_2O)_{12}Mo_8O_{27}]\cdot nH_2O$. (a) R = Gd, 750 °C, 2 h, first run (virgin alumina container). (b) R = Gd, 750 °C, 2 h, fourth run. (c) R = Gd, 750 °C, 4 h, third run. (d) R = Eu, 750 °C, 4 h, sixth run. (e) A single crystal of $Eu_2Mo_5O_{18}$.

Table 1. Crystal Data and Structure Refinement for $R_2Mo_5O_{18}$ and $R_6Mo_{12}O_{45}$ (R = Eu and Gd)

	$Eu_2Mo_5O_{18}$	$Gd_2Mo_5O_{18}$	$Eu_6Mo_{12}O_{45}$	$Gd_6Mo_{12}O_{45}$
fw	1071.61	1082.19	2783.01	2814.75
λ (Mo Kα), Å	0.71069	0.71069	0.71069	0.71069
space group (No.)	*Pbcn* (60)	*Pbcn* (60)	$P\bar{1}$ (2)	$P\bar{1}$ (2)
a, Å	19.2612(7)	19.246(1)	9.3867(4)	9.3409(3)
b, Å	9.4618(3)	9.4414(5)	10.9408(5)	10.8826(5)
c, Å	9.3779(3)	9.3446(4)	11.4817(5)	11.4377(5)
α, deg	90	90	104.194(2)	104.170(1)
β, deg	90	90	109.567(3)	109.288(4)
γ, deg	90	90	108.998(2)	109.266(2)
V, Å^3	1709.1(2)	1698.0(3)	963.93(8)	950.80(8)
Z	4	4	1	1
D_{calcd}, g/cm^3	4.164	4.233	4.794	4.916
μ, cm^{-1}	108.34	113.66	134.44	142.48
R^a (all data)	0.050	0.031	0.061	0.042
$R_w{}^b$ (all data)	0.068	0.039	0.097	0.067

[a] $R = \sum(F_o^2 - F_c^2)/\sum F_o^2$. [b] $R_w = \{\sum[w(F_o^2 - F_c^2)^2]/\sum[w(F_o^2)^2]\}^{1/2}$, where $w = [\sigma_c^2(F_o^2) + \{p(\mathrm{Max}(F_o^2, 0) + 2F_c^2)/3\}^2]^{-1}$, p = 0.04, 0.02, 0.05, and 0.05 for $Eu_2Mo_5O_{18}$, $Gd_2Mo_5O_{18}$, $Eu_6Mo_{12}O_{45}$, and $Gd_6Mo_{12}O_{45}$, respectively.

Table 2. Selected Bond Distances (Å) in $R_2Mo_5O_{18}$ (R = Eu and Gd)

	R = Eu	R = Gd		R = Eu	R = Gd
R−O2	2.344(5)	2.332(3)	Mo1−O6	1.734(5)	1.736(3)
R−O5	2.347(5)	2.339(3)	Mo1−O7	1.867(5)	1.874(3)
R−O3	2.349(4)	2.344(2)	Mo2−O3^{iii}	1.741(4)	1.738(3)
R−O1	2.363(5)	2.358(3)	Mo2−O3^{iv}	1.741(4)	1.738(3)
R−O9^{i} [a]	2.404(4)	2.402(3)	Mo2−O2	1.768(4)	1.775(3)
R−O6	2.426(4)	2.416(3)	Mo2−O2^{v}	1.768(4)	1.775(3)
R−O8^{ii}	2.437(4)	2.423(3)	Mo3−O4^{vi}	1.722(5)	1.721(3)
R−O4	2.514(5)	2.510(3)	Mo3−O5	1.723(5)	1.714(3)
Mo1−O9	1.719(4)	1.715(3)	Mo3−O1^{vii}	1.740(5)	1.732(3)
Mo1−O8	1.727(4)	1.727(3)	Mo3−O7^{viii}	1.862(5)	1.853(3)

[a] (i) $^1/_2 - x$, $^3/_2 - y$, $-^1/_2 + z$; (ii) x, $2 - y$, $-^1/_2 + z$; (iii) $1 - x$, $2 - y$, $-z$; (iv) x, $2 - y$, $^1/_2 + z$; (v) $1 - x$, y, $^1/_2 - z$; (vi) $1 - x$, y, $-^1/_2 - z$; (vii) x, $1 - y$, $-^1/_2 + z$; (viii) x, y, $-1 + z$.

Table 3. Selected Bond Distances (Å) in $R_6Mo_{12}O_{45}$ (R = Eu and Gd)

	R = Eu	R = Gd		R = Eu	R = Gd
R1−O3	2.302(7)	2.289(4)	Mo1−O7	1.775(6)	1.768(4)
R1−O1	2.365(6)	2.349(4)	Mo1−O8	1.790(6)	1.786(4)
R1−O2	2.365(5)	2.352(4)	Mo2−O12	1.748(6)	1.746(4)
R1−O6^{i} [a]	2.396(6)	2.385(4)	Mo2−O10	1.755(6)	1.749(4)
R1−O4	2.413(5)	2.377(4)	Mo2−O5	1.769(6)	1.766(4)
R1−O4^{ii}	2.462(6)	2.459(4)	Mo2−O11	1.787(6)	1.785(4)
R1−O5	2.502(6)	2.501(4)	Mo3−O13	1.740(6)	1.754(4)
R1−O5^{ii}	2.703(6)	2.673(5)	Mo3−O16	1.747(6)	1.738(4)
R2−O14	2.328(6)	2.311(4)	Mo3−O14	1.749(6)	1.751(5)
R2−O23^{iii}	2.371(5)	2.336(4)	Mo3−O4	1.801(6)	1.793(4)
R2−O10^{ii}	2.378(6)	2.362(4)	Mo4−O17^{i}	1.696(6)	1.710(4)
R2−O15	2.390(5)	2.382(4)	Mo4−O15^{ix}	1.719(6)	1.707(4)
R2−O21^{iv}	2.391(5)	2.363(4)	Mo4−O9	1.8580(6)	1.8574(5)
R2−O20^{v}	2.395(5)	2.375(4)	Mo4−O8	2.030(6)	2.025(4)
R2−O12^{iii}	2.423(6)	2.419(4)	Mo4−O11^{i}	2.091(6)	2.083(4)
R2−O7^{ii}	2.531(6)	2.531(4)	Mo4−O22^{x}	2.192(6)	2.200(5)
R3−O16	2.326(6)	2.319(4)	Mo5−O19	1.750(6)	1.756(4)
R3−O19	2.392(5)	2.368(4)	Mo5−O3^{v}	1.754(6)	1.754(4)
R3−O17	2.400(6)	2.359(4)	Mo5−O20	1.757(6)	1.749(5)
R3−O18	2.406(6)	2.400(4)	Mo5−O21	1.795(5)	1.796(4)
R3−O21^{vi}	2.415(5)	2.402(4)	Mo6−O22	1.744(6)	1.729(5)
R3−O23^{vii}	2.451(5)	2.443(4)	Mo6−O2^{xi}	1.746(5)	1.736(4)
R3−O13^{v}	2.469(6)	2.451(4)	Mo6−O23	1.816(5)	1.821(4)
R3−O7^{viii}	2.483(6)	2.456(4)	Mo6−O18	1.853(6)	1.849(4)
Mo1−O6	1.742(6)	1.740(4)	Mo6−O18^{vii}	2.278(6)	2.256(4)
Mo1−O1	1.754(6)	1.746(5)			

(i) $1 - x$, $-y$, $1 - z$; (ii) $-x$, $-y$, $1 - z$; (iii) x, y, $1 + z$; (iv) x, $1 + y$, $1 + z$; (v) $-x$, $-1 - y$, $1 - z$; (vi) $-1 - x$, $-2 - y$, $-z$; (vii) $-1 - x$, $-1 - y$, $-z$; (viii) $-1 + x$, $-1 + y$, z; (ix) $1 + x$, $1 + y$, z; (x) $1 + x$, $1 + y$, $1 + z$; (xi) $-1 + x$, $-1 + y$, $-1 + z$.

Results and Discussion

Decomposition and Crystallization Behavior. The europium and gadolinium polyoxomolybate precursors exhibited similar decomposition and crystallization behavior at 750 °C. The dark brown-green glassy product (Figure 1a) formed in a virgin container was $R_2O_3\cdot 6\sim 7MoO_3$ in composition. Figure 1b shows $Gd_2Mo_5O_{18}$ crystals (in the glassy phase) which were formed by reusing the same container four times (750 °C, 2 h). The effect of repeated use of an alumina container on enhancing crystallization was also pointed out for $Eu_4Mo_7O_{27}$ and $Eu_6Mo_{10}O_{39}$ which were obtained by decomposition of $[Eu_2(H_2O)_{12}Mo_8O_{27}]\cdot 6H_2O$ at 800 °C.[13] It has been suggested that nucleation occurs on the alumina

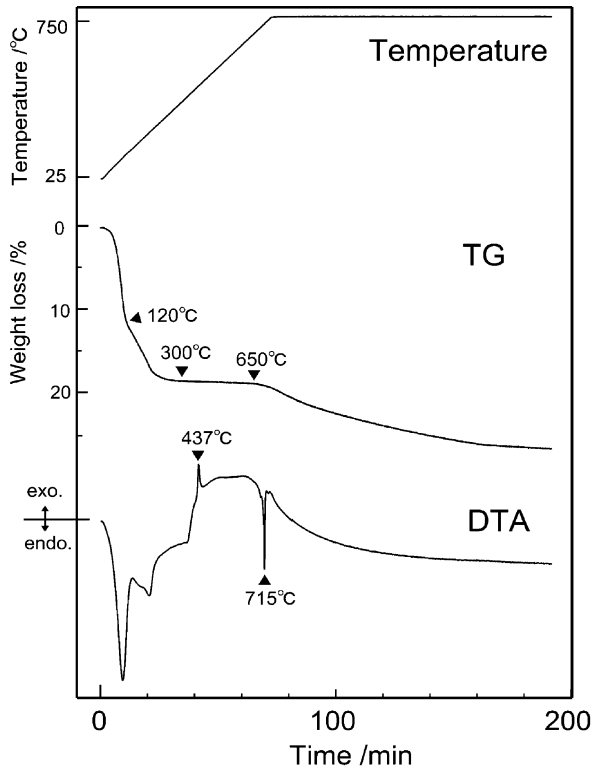

Figure 2. Thermal analysis of $[Gd_2(H_2O)_{12}Mo_8O_{27}]\cdot 8H_2O$. Top: temperature variation with time. Middle: TG curve. Bottom: DTA curve.

surface by exposure to the $R_2O_3-MoO_3$ melt. Figure 1e represents an example of a well-formed single crystal of $Eu_2Mo_5O_{18}$ with a size $1 \times 0.5 \times 0.2$ mm^3. Prolonged heating (longer than 4 h) at 750 °C led to formation of $R_6Mo_{12}O_{45}$ together with the $R_2Mo_5O_{18}$ phase (Figure 1c). Reuse of the same container also seems to promote the formation of $R_6Mo_{12}O_{45}$ as shown in Figure 1d, where all the crystals formed in the sixth run (750 °C, 4 h) were $R_6Mo_{12}O_{45}$.

Figure 2 displays the TG (middle) and DTA (bottom) curves for $[Gd_2(H_2O)_{12}Mo_8O_{27}]\cdot 8H_2O$ under the controlled temperature (top). There is a two-step dehydration process between room temperature (RT) and 300 °C corresponding to the elimination of $12H_2O$ (RT to 130 °C) and $8H_2O$ (130−300 °C) to form an amorphous $Gd_2Mo_8O_{27}$ phase. The sharp exothermic peak at ∼437 °C may be the crystallization of the amorphous phase, because several XRD peaks appear above this temperature (structure is unknown). Melting of the sample occurs at 715 °C with an accompanying sharp endothermic peak. A gradual weight loss with a broad endothermic curve at >700 °C is due to the vaporization of MoO_3. The final products treated at 750 °C for 2 and 4 h were crystals of $Gd_2Mo_5O_{18}$ and $Gd_6Mo_{12}O_{45}$ (with the glassy phase), respectively. It was concluded that $R_6Mo_{12}O_{45}$ is formed from $R_2Mo_5O_{18}$ with the loss of MoO_3, because we observed that a firing of single crystals of $R_2Mo_5O_{18}$ at 750 °C gave polycrystalline $R_6Mo_{12}O_{45}$. The crystallization of $R_2Mo_5O_{18}$ and the transformation into $R_6Mo_{12}O_{45}$ take place gradually, exhibiting no endo- nor exothermic peak (Figure 2, bottom). These results can be described schematically as follows:

$$[Gd_2(H_2O)_{12}Mo_8O_{27}]\cdot 8H_2O \rightarrow Gd_2Mo_8O_{27}(a) + 20H_2O \text{ (RT to 300 °C)}$$

$$Gd_2Mo_8O_{27}(a \rightarrow c) \text{ (437 °C)}$$

$$Gd_2Mo_8O_{27}(c \rightarrow l) \text{ (715 °C)}$$

$$Gd_2Mo_8O_{27}(l) \rightarrow Gd_2Mo_5O_{18}(c) + 3MoO_3 \text{ (750 °C)}$$

$$3Gd_2Mo_5O_{18}(c) \rightarrow Gd_6Mo_{12}O_{45}(c) + 3MoO_3 \text{ (750 °C)}$$

where c, a, and l denote crystalline, amorphous, and liquid phases, respectively. The decomposition behavior of $[Eu_2(H_2O)_{12}Mo_8O_{27}]\cdot 6H_2O$ was similar to that of the Gd analogue (data are available as Supporting Information), except for an additional exothermic peak at 558 °C due to the second phase transition of the crystalline phase, that is, $Eu_2Mo_8O_{27}$-(c → c′). Melting of $Eu_2Mo_8O_{27}$(c′) occurs at 708 °C.

Structure of $R_2Mo_5O_{18}$. The europium and gadolinium compounds of $R_2Mo_5O_{18}$ are isomorphous and crystallize in an orthorhombic form, *Pbcn*. The crystal structure consists of $\{MoO_4\}$ tetrahedra and square-antiprismatic O-coordinated R atoms (Figure 3a). The $\{Mo(1)O_4\}$ and $\{Mo(3)O_4\}$ tetrahedra share a corner at O(7), forming a $\{Mo_2O_7\}$ group (Figure 3b) with a nearly linear Mo(1)−O(7)−Mo(3) angle (173.4(4)° for R = Eu; 173.5(2)° for R = Gd). The Mo(1)−O(7) and Mo(3)−O(7) bond lengths are longer than other Mo−O distances. The $\{Mo(2)O_4\}$ tetrahedron, which is isolated from other molybdate groups, is attached by four $\{RO_8\}$ square-antiprisms through all four O atoms. Figure 3c represents the distorted square-antiprismatic coordination of the $\{RO_8\}$ group, where [O(1), O(4), O(5), O(9)] and [O(2), O(3), O(8), O(6)] define the two squares. The $\{RO_8\}$ group is attached by eight $\{MoO_4\}$ tetrahedra through all eight O atoms and is thereby separated from the other $\{RO_8\}$ groups.

It should be noted that an R atom has 12 neighboring R atoms within a narrow range of R···R distances (6.0831(6)−7.0389(4) Å for R = Eu; 6.0735(4)−7.0257(3) Å for R = Gd). These 12 R atoms form an approximate cuboctahedron (Figure 3d). In the lattice, a cuboctahedron is connected to six adjacent equivalent polyhedra through its six square-faces (only a pair of the polyhedra is shown in Figure 3d). In other words, the R atoms are distributed uniformly in the lattice of $R_2Mo_5O_{18}$.

A rare earth molybdate with a $R_2O_3\cdot 5MoO_3$ composition was reported for R = La.[21] However, the results of a later investigation of the $nLa_2O_3\cdot mMoO_3$ system[22] showed no existence of the $La_2O_3\cdot 5MoO_3$ phase. The powder X-ray diffraction pattern reported for $La_2O_3\cdot 5MoO_3$[21] was not consistent with that for $R_2Mo_5O_{18}$ (R = Eu and Gd) which was calculated on the basis of the single-crystal X-ray crystallographic data, suggesting that $La_2O_3\cdot 5MoO_3$ is not

(21) Get'man, E. I.; Mokhosoev, M. V. *Inorg. Mater.* **1968**, *4*, 1354.
(22) Fournier, J. P.; Fournier, J.; Kohlmuller, R. *Bull. Soc. Chim. Fr.* **1970**, 4277.

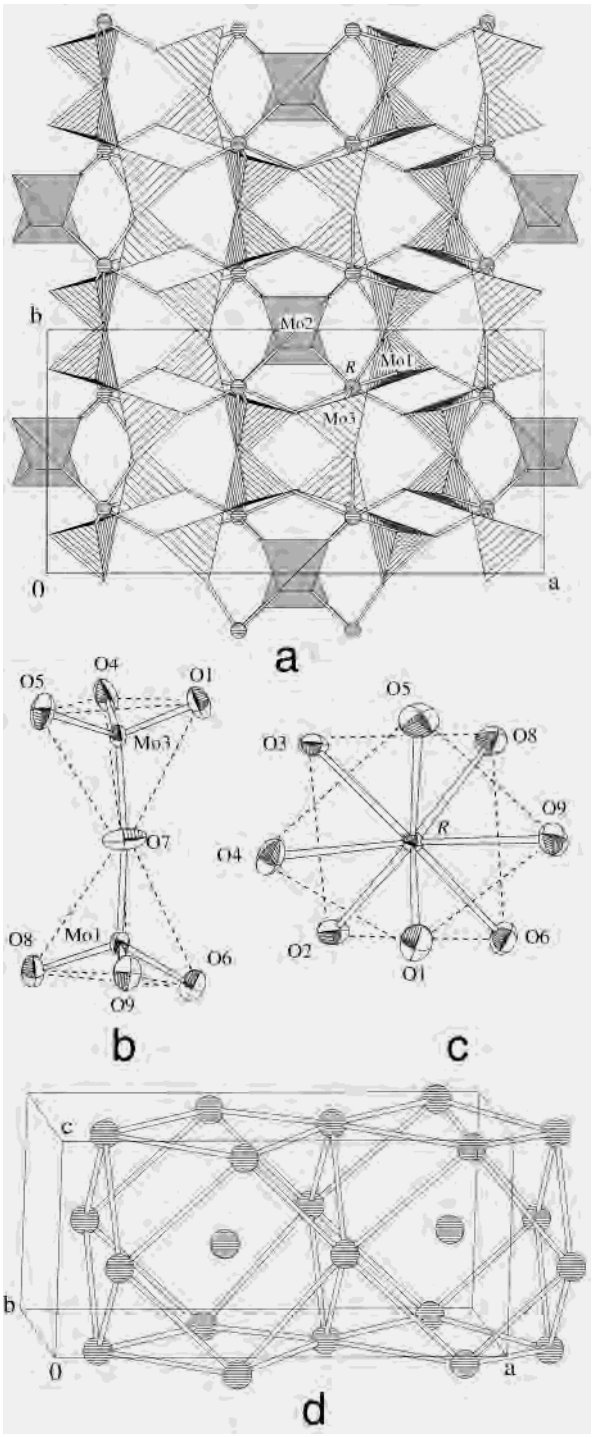

Figure 3. (a) Crystal structure of $R_2Mo_5O_{18}$ projected onto the (001) plane. The hatched spheres are R atoms. The $\{MoO_4\}$ groups centered by Mo(2) and Mo(1,3) are denoted by shaded and hatched tetrahedra, respectively. (b) $\{Mo_2O_7\}$ group. (c) $\{RO_8\}$ square-antiprism. (d) Two face-sharing cuboctahedra, each of which consists of a central R and surrounding 12 R atoms. The thermal ellipsoids in b and c are of the Eu compound.

isostructural with $R_2Mo_5O_{18}$ (R = Eu and Gd) in this study. In the equilibrium study for the nGd$_2$O$_3$·mMoO$_3$ system,[23] n:m = 1:1, 1:3, 1:4, and 1:6 phases were found, but no 1:5 phase has been reported. On the other hand, only n:m = 1:1, 1:3,[11] and recently discovered 2:7 and 3:10,[13] ratios have been observed in the nEu$_2$O$_3$·mMoO$_3$ system. Our attempt to prepare $Eu_2Mo_5O_{18}$ by firing (650−750 °C) a stoichiometric mixture of $Eu_2O_3 + 5MoO_3$ resulted in the formation of $Eu_6Mo_{12}O_{45}$ with the loss of MoO_3. In conclusion, $R_2Mo_5O_{18}$ (R = Eu and Gd) is the first example of a structurally determined m:n = 1:5 phase in the nR$_2$O$_3$·mMoO$_3$ system.

Structure of $R_6Mo_{12}O_{45}$. The europium and gadolinium compounds of $R_6Mo_{12}O_{45}$ are isomorphous and crystallize in a triclinic form, $P\bar{1}$. One may point out that $R_6Mo_{12}O_{45}$ is stoichiometrically equivalent with $R_2Mo_4O_{15}$. However, because the crystallographically asymmetric unit is $R_3Mo_6O_{22.5}$, this compound can be better formulated as $R_6Mo_{12}O_{45}$ (=$2R_3Mo_6O_{22.5}$). The crystal structure comprises four $\{Mo(1,2,3,5)O_4\}$ tetrahedra, one $\{Mo(6)O_5\}$ square pyramid, one $\{Mo(4)O_6\}$ octahedron, and three R(1−3) atoms (Figure 4a). The $\{Mo(4)O_6\}$ and symmetry-related $\{Mo(4^*)O_6\}$ octahedra share a corner at the O(9) atom, forming a $\{Mo_2O_{11}\}$ group with an ideally linear Mo(4)−O(9)−Mo(4*) angle (180°) (Figure 4b). The $\{Mo(6)O_5\}$ square pyramid (basal plane of [O(18), O(22), O(23), O(18′)] and apical O(2) atom) can also be viewed as an O(18′)-capped $\{Mo(6)O_4\}$ tetrahedron because of the long Mo(6)−O(18′) distance (R = Eu, 2.278(6) Å; R = Gd, 2.256(4) Å) compared with other Mo−O distances (1.729(5)−1.853(6) Å). Two $\{Mo(6)O_5\}$ polyhedra share the O(18)···O(18′) edge, to form a $\{Mo_2O_8\}$ group (Figure 4b). These dimeric $\{Mo_2O_{11}\}$ and $\{Mo_2O_8\}$ groups are connected alternately by corner-sharing through the O(22) atom, giving rise to a polymeric $\{Mo_4O_{17}\}_\infty$ chain running along the a-axis (Figure 4b). The $\{Mo(1)O_4\}$ and $\{Mo(2)O_4\}$ tetrahedra are attached to the molybdate chain at the O(11) and O(15) atoms. The $\{Mo(3)O_4\}$ and $\{Mo(5)O_4\}$ tetrahedra are isolated from other molybdate polyhedra.

All the R atoms achieve square-antiprismatic coordination by eight O atoms. Unlike the isolated distribution of the $\{RO_8\}$ polyhedra in $R_2Mo_5O_{18}$, the $\{RO_8\}$ groups in $R_6Mo_{12}O_{45}$ are connected by face-sharing. The $\{R(2)O_8\}$ and $\{R(3)O_8\}$ polyhedra share a plane defined by O(7), O(21), and O(23) with an R(2)···R(3) distance of 3.6798(5) and 3.6484(4) Å for R = Eu and Gd, respectively (Figure 4c). Similar triply oxo-bridged R pairs were found for $R_2Mo_4O_{15}$ (R = La,[12] Ce,[24] Pr[25]), $Eu_4Mo_7O_{27}$, and $Eu_6Mo_{10}O_{39}$.[13] It is interesting to note that $\{R(1)O_8\}$ and symmetry-related $\{R(1')O_8\}$ square-pyramids are fused by sharing the [O(4), O(4′), O(5), O(5′)] square-face to form a $\{R_2O_{12}\}$ group, which induces an extremely short R(1)···R(1′) distance (3.4741(7) and 3.4502(6) Å for R = Eu and Gd, respectively) (Figure 4d). To our knowledge, both the geometry of the $\{R_2O_{12}\}$ group and the short $R^{3+}\cdots R^{3+}$ separation (<3.5 Å) are the first examples among all rare earth oxide compounds. Disordering between R(1) and R(1′) is unlikely because of the normal thermal parameter (B_{eq} = 0.700(6)−0.713(7) Å^2) for R(1), which is comparable to those (B_{eq} = 0.609(6)−0.655(7) Å^2) for R(2) and R(3). The empirical valence

(23) Megumi, K.; Yumoto, H.; Ashida, S.; Akiyama, S.; Furuhata, Y. *Mater. Res. Bull.* **1974**, *9*, 391.
(24) Fallon, G. D.; Gatehouse, B. M. *J. Solid State Chem.* **1982**, *44*, 156.
(25) Efremov, V. A.; Davydova, N. N.; Trunov, V. K. *Russ. J. Inorg. Chem.* **1988**, *33*, 1729.

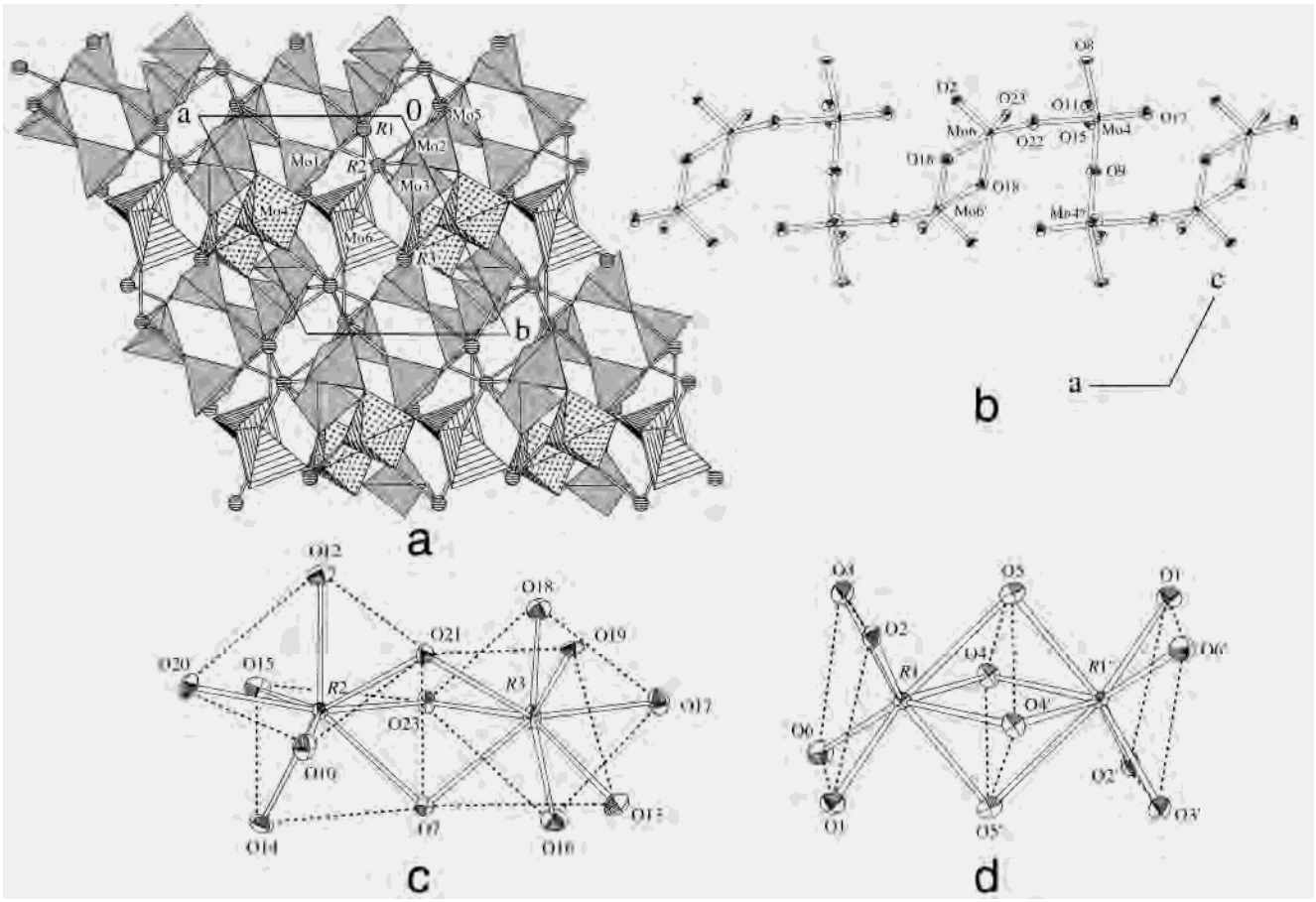

Figure 4. (a) Crystal structure of $R_6Mo_{12}O_{45}$ viewed parallel to the *c*-axis. The hatched spheres are R atoms. The crosshatched and line-hatched polyhedra are $\{Mo(4)O_6\}$ and $\{Mo(6)O_5\}$ groups, respectively. The shaded tetrahedra are $\{Mo(1,2,3,5)O_4\}$ groups. (b) $\{Mo_2O_{17}\}_\infty$ chain viewed along the *b*-axis. (c) $\{R_2O_{13}\}$ group. (d) $\{R_2O_{12}\}$ group. Squares in $\{RO_8\}$ square-antiprisms are drawn with broken lines in c and d. The thermal ellipsoids in b, c, and d are of the Eu compound.

calculation[26] for R(1) gave reasonable values (3.1 for R = Eu; 3.2 for R = Gd) for the trivalent R^{3+} cation. In the $\{R(1)O_8\}$ moiety, the R center is significantly displaced toward the [O(1), O(2), O(3), O(6)] square: distances from R to the least-squares plane of the [O(1), O(2), O(3), O(6)] square are 1.054(4)−1.055(3) Å, while those to the [O(4), O(4′), O(5), O(5′)] square are 1.720(7)−1.732(8) Å. This is due to the strong electrostatic repulsion between the short R(1)···R(1′) separation.

In the equilibrium study of the $n Gd_2O_3 \cdot m MoO_3$ system, the existence of the $n:m = 1:4$ phase has been assumed using DTA and powder X-ray diffractometry,[23] but its structure is unknown because no single crystal is obtained by the conventional stoichiometric synthesis. Figure 5 shows the powder XRD pattern of $Gd_2O_3 \cdot 4MoO_3$ reported by Alekseev et al.[27] and the calculated pattern of $Gd_6Mo_{12}O_{45}$ based on the structural analysis. One may notice that most of the observed peaks (Figure 5a) agree with the intense calculated peaks (Figure 5b). This result suggests strongly that the previously reported $Gd_2O_3 \cdot 4MoO_3$ (=$Gd_2Mo_4O_{15}$) is actually identical to $Gd_6Mo_{12}O_{45}$ (=$3Gd_2Mo_4O_{15}$) found in this study.

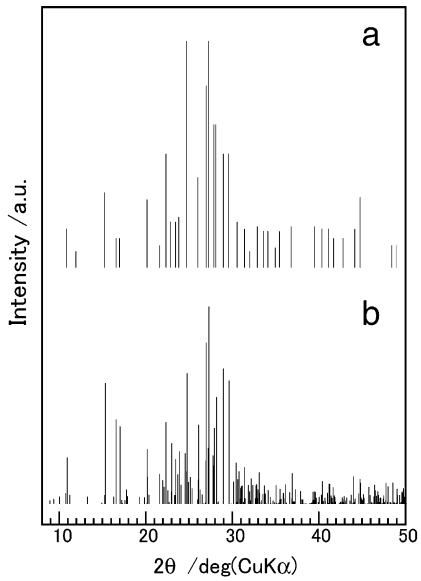

Figure 5. XRD patterns of (a) $Gd_2O_3 \cdot 4MoO_3$ reported by Alkseev et al.[27] and (b) $Gd_6Mo_{12}O_{45}$ calculated on the basis of the single-crystal X-ray structural determination.

Three different structures have been reported for $R_2Mo_4O_{15}$: (i) R = La,[12] (ii) R = Ce [24] and Pr,[25] and (iii) R = Tb [14] and Ho,[15] which include hexameric $\{Mo_6O_{22}\}$, polymeric $\{Mo_4O_{14}\}_\infty$, and tetrameric $\{Mo_4O_{15}\}$ units, respec-

(26) Brown, I. D. *Structure and Bonding in Crystals*; O'Keeffe, M., Navrotsky A., Eds.; Academic Press: New York, 1980; Vol. II, pp 1−30.
(27) Alekseev, E. P.; Get'man, E. I.; Koshcheev, G. G.; Mokhosoev, M. V. *Russ. J. Inorg. Chem.* **1969**, *14*, 1558.

tively. The polymeric $\{Mo_4O_{14}\}_\infty$ unit in (ii) is composed of two edge-shared $\{MoO_6\}$ octahedra which are linked by two $\{MoO_4\}$ tetrahedra by corner-sharing, exhibiting no similarity to the $\{Mo_4O_{17}\}_\infty$ chain (Figure 4b) in $R_6Mo_{12}O_{45}$.

Conclusions

Single crystals of novel $R_2Mo_5O_{18}$ and $R_6Mo_{12}O_{45}$ (R = Eu and Gd) have been obtained by thermal decomposition of $[R_2(H_2O)_{12}Mo_8O_{27}]\cdot nH_2O$, and their structures have been characterized. The TG-DTA and X-ray diffractometry for the precursor revealed that $R_2Mo_5O_{18}$ crystallizes in a melt of the dehydrated precursor $R_2Mo_8O_{27}$, and $R_2Mo_5O_{18}$ is transformed to $R_6Mo_{12}O_{45}$ in the solid state, both of which occur at 750 °C with the loss of MoO_3. It is difficult to prepare $R_2Mo_5O_{18}$ by firing a stoichiometric mixture of R_2O_3 and MoO_3 at 750 °C, because $R_2Mo_5O_{18}$ is metastable and readily converted to $R_6Mo_{12}O_{45}$.

Both structures consist of $\{RO_8\}$ square-antiprisms and $\{MoO_n\}$ polyhedra. In $R_2Mo_5O_{18}$, an $\{RO_8\}$ polyhedron is attached by only molybdate groups, being isolated from adjacent $\{RO_8\}$ groups in the crystal lattice. All the $\{RO_8\}$ square-antiprisms in $R_6Mo_{12}O_{45}$ are connected by face-sharing to form dimeric $\{R_2O_{13}\}$ and $\{R_2O_{12}\}$ groups. The latter unusual $\{R_2O_{12}\}$ group is achieved by sharing a square-face via four bridging O atoms with a very short R···R separation (3.4741(7)−3.4502(6) Å). It is strongly suggested that $Gd_6Mo_{12}O_{45}$ is equivalent to $Gd_2Mo_4O_{15}$ which has been described by Alekseev [27] and Megumi.[23]

We conclude that the thermal decomposition of $[R_2(H_2O)_{12}Mo_8O_{27}]\cdot nH_2O$ is of great advantage in the investigation of phases, crystal growths, and structures in the $mR_2O_3\cdot nMoO_3$ system.

Acknowledgment. This research was supported in part by Grant-in-Aid for Scientific Research (10304055 and 1274036) from the Ministry of Education, Science, Sports, and Culture.

Supporting Information Available: X-ray crystallographic data for $R_2Mo_5O_{18}$ and $R_6Mo_{12}O_{45}$ (R = Eu and Gd) in CIF format, IR spectra, and a figure on TG-DTA for $[Eu(H_2O)_{12}Mo_8O_{27}]\cdot 6H_2O$. This material is available free of charge via the Internet at http://pubs.acs.org.

IC025697Z